Double phi-Step theta-Scanning Technique for Spherical Near-Field Antenna Measurements

Double ϕ-Step θ-Scanning Technique for Spherical Near-Field Antenna Measurements

Laitinen, Tommi

Published in:
IEEE Transactions on Antennas and Propagation

Link to article, DOI:
10.1109/TAP.2008.923308

Publication date:
2008

Document Version
Publisher's PDF, also known as Version of record

Double ϕ-Step θ-Scanning Technique for Spherical Near-Field Antenna Measurements

Tommi Laitinen

***Abstract*—Probe-corrected spherical near-field antenna measurements with an arbitrary probe set certain requirements on an applicable scanning technique. The computational complexity of the general high-order probe correction technique for an arbitrary probe, that is based on the ϕ scanning, is $O(N^4)$, where N is proportional to the radius of the antenna under test (AUT) minimum sphere in wavelengths. With the present knowledge, the computational complexity of the probe correction for arbitrary probes in the case of the θ scanning is $O(N^6)$, which is typically not acceptable. This paper documents a specific double ϕ-step θ-scanning technique for spherical near-field antenna measurements. This technique not only constitutes an alternative spherical scanning technique, but it also enables formulating an associated probe correction technique for arbitrary probes with the computational complexity of $O(N^4)$ while the possibility for the exploitation of the advantages of the θ scanning are maintained.**

***Index Terms*—Antenna measurement, probe correction, spherical near field.**

I. Introduction

SPHERICAL near-field antenna measurement is a well-founded technique for the antenna pattern characterization [1]. Inclusion of the probe correction in the near-field to far-field transformation enables accurate determination of the far field [2].

Traditionally, the first-order ($\mu = \pm 1$) probe correction technique [1] has been applied for the probe correction, and it leads to the computational complexity of $O(N^3)$ in the probe correction. Here N is proportional to the radius of antenna under test (AUT) minimum sphere in wavelengths. Recently, a probe correction technique for odd-order ($\mu = \pm 1, \pm 3 \ldots$) probes, for which the computational complexity is $O(N^4)$, has been presented in [3].

The first and odd-order probe correction techniques rely on the assumption that the azimuthal radiation pattern of the probe contains only either first-order or odd-order variations, respectively. Good examples of first and odd-order probes are open-ended circular and rectangular waveguide probes, respectively, excited with their fundamental waveguide modes. The wider the required bandwidth for the probe is, the more difficult it practically becomes to construct a probe that provides precisely the first-order or odd-order azimuthal variation of the probe pattern assumed by the first and odd-order probe correction techniques. For this reason, in practice, to cover, e.g., the 1–3 GHz frequency range, it has been typical to use several waveguide probes. However, significant savings in the measurement time could be gained by using only one probe covering the whole frequency range.

A natural way to overcome the necessity for precise manufacturing of a probe is to apply a more general probe correction technique. Two known techniques for this purpose are the iterative [4] and the general high-order [5] probe correction techniques. A drawback of the iterative technique, though being computationally efficient, is that its applicability range is not precisely known [6]. Instead, although being less computationally efficient, the fact that the general high-order probe correction technique is applicable for (almost) arbitrary probes makes it attractive.

A complete antenna pattern characterization procedure based on the general high-order probe correction technique has been recently developed for the DTU-ESA Spherical Near-Field Antenna Test Facility [7] within a project funded by the European Space Agency [8]. This work has shown that the use of an arbitrary probe sets certain specific requirements on an applicable scanning technique [9], which do not have to be taken into consideration if the probe correction is not included [10], or if the simplification of assuming a first-order probe is made [11] [12]. For instance, in the case of the ϕ scanning the computational complexity of $O(N^4)$ in the probe correction for arbitrary probes is reached, which is sufficient for a major part of the antenna measurement projects. In the case of the θ scanning, the computational complexity becomes $O(N^6)$ [13], and this is typically not acceptable. A possibility for the θ scanning would, however, be useful, because it is known to have certain advantages over the ϕ scanning [1].

The purpose of this paper is to introduce a specific double ϕ-step θ-scanning technique for spherical near-field antenna measurements. While being applicable also with a first or odd-order probe, the technique is shown to be particularly beneficial in the case of an arbitrary probe for which it enables formulating a probe correction technique with the computational complexity of $O(N^4)$ and maintaining the possibility for the exploitation of the advantages of the θ scanning. Compared to the usual θ-scanning technique [1], the application of the double ϕ-step θ-scanning technique does not practically increase the measurement time.

The background theory for the probe-corrected spherical near-field antenna measurements is presented in Section II. The double ϕ-step θ-scanning technique, and the probe correction technique based on this scanning technique, are presented in Section III. Validation of the technique is presented in Section IV, and conclusions in Section V.

Manuscript received December 12, 2006; revised December 18, 2007.

The author was with the Technical University of Denmark (DTU), Ørsteds Plads, DK-2800 Kgs. Lyngby, Denmark. He is now with the Radio Laboratory, Helsinki University of Technology (TKK), Espoo FI-02015, Finland (e-mail: tommi.laitinen@tkk.fi).

Digital Object Identifier 10.1109/TAP.2008.923308

II. Background Theory

A. Measurement Geometry

The spherical antenna measurement geometry is presented in Fig. 1. The (x, y, z) and (x', y', z') are the Cartesian coordinates of the AUT and the probe coordinate systems, respectively. The (r, θ, ϕ) are the spherical coordinates of the AUT coordinate system. The measurement distance r is the distance between the origins of the AUT and the probe coordinate systems. The AUT and probe minimum spheres are centered in the AUT and the probe coordinate systems, respectively. The χ is the probe orientation angle such that for $\chi = 0$ and $\chi = \pi/2$ the x' axis coincides with the θ and ϕ unit vectors of the AUT coordinate system, respectively.

B. Transmission Formula

The transmission formula [1], that expresses the signal received by the probe (w) as a function of the unknown coefficients Q_{smn}, can be written as

$$w(r,\chi,\theta,\phi) = \sum_{s=1}^{2}\sum_{n=1}^{N}\sum_{m=-\min(M,n)}^{\min(M,n)} Q_{smn}e^{im\phi} \times \sum_{\mu=-\min(n,\mu_{\max})}^{\min(n,\mu_{\max})} P_{s\mu n}(kr)e^{i\mu\chi}d^{n}_{\mu m}(\theta) \quad (1)$$

where Q_{smn} are the spherical vector wave coefficients of the spherical wave expansion of the AUT field, the terms $e^{im\phi}$, $e^{i\mu\chi}$ and $d^{n}_{\mu m}(\theta)$ are the three rotation functions of the spherical vector wave functions, and the probe response constants are

$$P_{s\mu n}(kr) = \frac{1}{2}\sum_{\nu=\max(1,|\mu|)}^{\nu_{\max}}\sum_{\sigma=1}^{2} C^{sn(3)}_{\sigma\mu\nu}(kr)R^{(p)}_{\sigma\mu\nu} \quad (2)$$

where $C^{sn(3)}_{\sigma\mu\nu}(kr)$ are the translation coefficients, and $R^{(p)}_{\sigma\mu\nu}$ are the probe receiving coefficients [1]. As in [1], the integers N and M are the truncation numbers for the n and m summations of the spherical wave expansion of the AUT field [1], respectively, and proportional to the radii of the AUT minimum sphere and cylinder (shown in Fig. 1) in wavelengths, respectively. Similarly, the integers $\nu_{\max}$ and $\mu_{\max}$ are the truncation numbers for the ν and μ summations of the spherical wave expansion of the probe field, respectively, and proportional to the radii of the probe minimum sphere and cylinder (shown in Fig. 1) in wavelengths [1], respectively.

III. Double ϕ-Step θ-Scanning Technique and Probe Correction Technique for Arbitrary Probes

The near-field to far-field transformation including the probe correction is accomplished by solving the transmission formula (1) for Q_{smn}, and by calculating the far field from the spherical wave expansion of the AUT field. The probe receiving coefficients in (2) are known from a separate probe pattern calibration measurement. A spherical near-field measurement for the AUT provides the necessary probe signals in the left-hand side of the transmission formula.

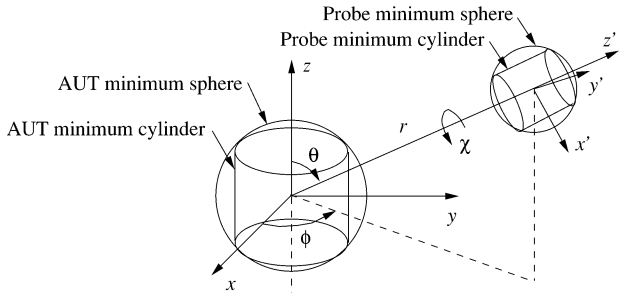

Fig. 1. Measurement geometry.

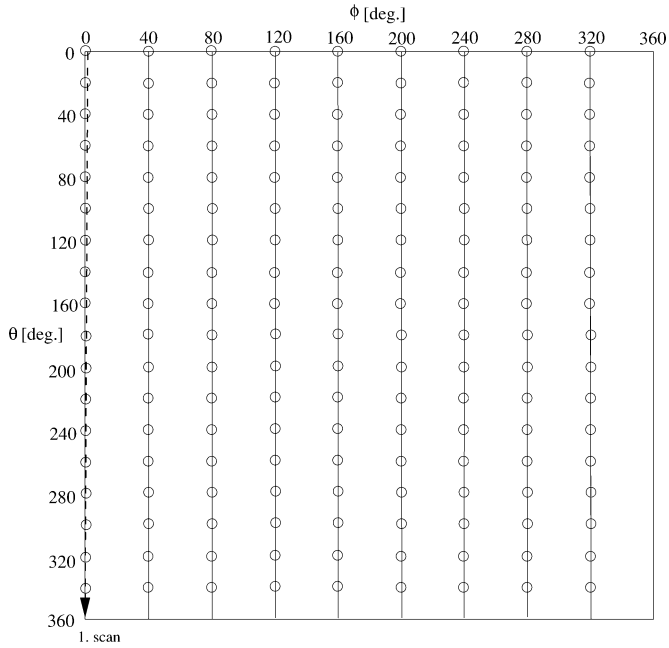

Fig. 2. Illustration of the measurement directions in the angular region $0 \leq \theta \leq 2\pi$ for the double ϕ-step θ-scanning technique. In this example case the double ϕ step is $2\delta\phi = 40°$, $N'_\phi = 9$, $\delta\theta = 20°$, and $N'_\theta = 18$.

In the case of an arbitrary probe, the possibility for exploiting the orthogonality of $e^{im\phi}$ in solving the transmission formula (1) place the ϕ and θ-scanning techniques in an essentially different position [9]. In the case of the ϕ scanning, this orthogonality can be exploited, and the computational complexity of $O(N^4)$ in solving the transmission formula (i.e., in performing the probe correction) is reached. With the present knowledge, in the case of the θ scanning, the orthogonality of $e^{im\phi}$ cannot be exploited, and the computational complexity of the probe correction becomes $O(N^6)$.

A specific double ϕ-step θ-scanning technique, and a probe correction technique associated with it, will be presented in this section. It will be shown that the double ϕ-step θ-scanning technique provides a possibility to indirectly exploit the orthogonality of $e^{im\phi}$, and to reach the computational complexity of $O(N^4)$ in the probe correction for arbitrary probes.

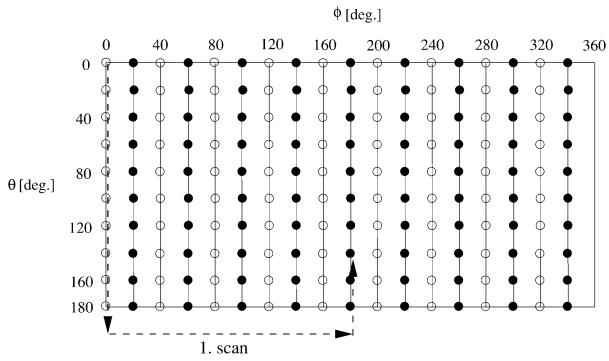

Fig. 3. Illustration of the measurement directions and the corresponding probe orientation angles in the angular region $0 \leq \theta \leq \pi$ (upper sphere) for the double ϕ-step θ-scanning technique. The probe orientation angle is χ for $\phi = 0, 2\delta\phi, 4\delta\phi \ldots 2\pi - 2\delta\phi$ (white nodes), and $\chi + \pi$ for $\phi = \delta\phi, 3\delta\phi, \ldots 2\pi - \delta\phi$ (black nodes).

A. Double ϕ-Step θ-Scanning Technique

In the double ϕ-step θ-scanning technique the stepping is performed in ϕ for $0 \leq \phi \leq 2\pi - 2\delta\phi$ in steps of $2\delta\phi$, where $2\delta\phi$ is the double ϕ step. The total number of ϕ angles is N'_ϕ, and, importantly, N'_ϕ must be an odd integer. For each fixed ϕ, the scanning is performed in θ for $0 \leq \theta \leq 2\pi - \delta\theta$, and the samples become available in the intervals of $\delta\theta$. The total number of samples in θ for $0 \leq \theta \leq 2\pi - \delta\theta$ is N'_θ. It is assumed here for simplicity that N'_θ is an even integer. A possible scanning grid for the double ϕ-step θ-scanning technique is illustrated in Fig. 2, where the double ϕ step is $2\delta\phi = 40°$, $N'_\phi = 9$, the θ interval is $\delta\theta = 20°$, and $N'_\theta = 18$.

In each measurement direction, the samples are gathered for the probe orientation angles $\chi = \chi_1$ and $\chi = \chi_2$, and it is assumed here, that $\chi_1 = 0$ and $\chi_2 = \pi/2$. The measurement distance r is the same in each measurement direction.

The measurement directions, that are shown in Fig. 2 in the angular region $0 \leq \theta \leq 2\pi$ (2-sphere), are now mapped to the corresponding directions in the angular region $0 \leq \theta \leq \pi$ (upper sphere), and illustrated in Fig. 3, where the probe orientation angles χ and $\chi + \pi$ are depicted with white and black nodes, respectively. Importantly, due to the requirement that N'_ϕ is an odd integer, the measurement directions in the upper sphere interleave in ϕ, so that for every second ϕ angle the probe orientation angle is χ (white nodes), and for the other ϕ angles it is $\chi + \pi$ (black nodes).

The total number of measurement angles in ϕ in the upper sphere in the interval $0 \leq \phi \leq 2\pi - \delta\phi$ is denoted N_ϕ, and the total number of measurement angles in θ in the interval $0 \leq \phi \leq \pi$ is denoted N_θ. The following relations then hold: $N_\phi = 2N'_\phi$, and $N_\theta = N'_\theta/2 + 1$. The upper-sphere samples are thus available in the measurement directions $\phi = (j-1)\delta\phi$ and $\theta = (l-1)\delta\theta$ for each possible index pair (j, l) for $j = 1 \ldots N_\phi$ and $l = 1 \ldots N_\theta$. For the example scanning grid illustrated in Fig. 3 $N_\phi = 18$, and $N_\theta = 10$.

For comparison, while the stepping is performed from 0 to $\pi - \delta\phi$ in steps of $\delta\phi$ in the θ-scanning technique [1], it is performed from 0 to $2\pi - 2\delta\phi$ in steps of $2\delta\phi$ in the double ϕ-step θ-scanning technique. The number of steps in ϕ thus remains the same for the two scanning techniques. The measurement directions remain the same as well, and thus the only essential difference between the two techniques is with the probe orientation angles in the upper sphere.

B. Probe Correction Technique

The probe correction technique based on the double ϕ-step θ-scanning technique is presented in this section. The sampling criteria is presented first in Section III-B.1. The two parts of the probe correction technique: 1) the indirect exploitation of the orthogonality of $e^{im\phi}$, and 2) the matrix inversions, will then be presented in Sections III-B.2 and III-B.3, respectively.

1) Sampling Criteria: The number required ϕ angles for the double ϕ-step θ-scanning technique, N'_ϕ, must be chosen as follows:

$$N'_\phi \geq M + 1 \tag{3}$$

and, as previously mentioned, this must be an odd integer. The number of samples in θ, N'_θ, must be chosen as follows:

$$N'_\theta \geq 2(N + n_3) \tag{4}$$

where the right choice of the integer n_3, that is related to the degree of over-sampling, depends on the application. According to the author's experience, n_3 should be greater than or equal to 1, and can be chosen from the range $1 \leq n_3 \leq 10$.

2) Indirect Exploitation of the Orthogonality of $e^{im\phi}$: As illustrated in Fig. 3, the probe orientation angles in the double ϕ-step θ-scanning technique in the upper sphere are χ and $\chi+\pi$. By interchanging the n and m summations of the transmission formula (1), the received signals for these two probe orientation angles are first rewritten in terms of Fourier expansions as follows:

$$w(r, \chi, \theta, \phi) = \sum_{m=-M}^{M} \left(w_m^{(e)}(r, \chi, \theta) + w_m^{(o)}(r, \chi, \theta) \right) e^{im\phi} \tag{5}$$

$$w(r, \chi + \pi, \theta, \phi) = \sum_{m=-M}^{M} \left(w_m^{(e)}(r, \chi, \theta) - w_m^{(o)}(r, \chi, \theta) \right) e^{im\phi} \tag{6}$$

where the Fourier coefficients of the even and odd-order signals are

$$w_m^{(e)}(r, \chi, \theta) = \sum_{n=n_0}^{N} \sum_{s=1}^{2} Q_{smn} g_{smn}^{(e)}(r, \chi, \theta) \tag{7}$$

$$w_m^{(o)}(r, \chi, \theta) = \sum_{n=n_0}^{N} \sum_{s=1}^{2} Q_{smn} g_{smn}^{(o)}(r, \chi, \theta) \tag{8}$$

respectively. Here $n_0 = \max(1, |m|)$, and

$$g^{(e)}_{smn}(r,\chi,\theta) = \sum_{\substack{\mu=-\mu_1 \\ (\mu\ \text{even})}}^{\mu_1} P_{s\mu n}(kr) e^{i\mu\chi} d^n_{\mu m}(\theta) \tag{9}$$

$$g^{(o)}_{smn}(r,\chi,\theta) = \sum_{\substack{\mu=-\mu_1 \\ (\mu\ \text{odd})}}^{\mu_1} P_{s\mu n}(kr) e^{i\mu\chi} d^n_{\mu m}(\theta). \tag{10}$$

The following discrete signal is now formed for each index pair (p,l):

$$\bar{w}_{pl} = [w_1(r,\chi_p,\theta_l,\phi_j) | j = 1 \dots N_\phi] \tag{11}$$

where

$$w_1(r,\chi_p,\theta_l,\phi_j) = \begin{cases} w(r,\chi_p,\theta_l,(j-1)\delta\phi) & (j\ \text{odd}) \\ -w(r,\chi_p+\pi,\theta_l,(j-1)\delta\phi) & (j\ \text{even}). \end{cases} \tag{12}$$

The components $w_1(r,\chi_p,\theta_l,\phi_j)$ for $j = 1,3,5 \dots N_\phi - 1$ are thus samples of the received signal in the upper sphere for $\phi = 0, 2\delta\phi, 4\delta\phi \dots 2\pi - 2\delta\phi$, respectively, and represent the samples of the signal in the left-hand side of (5). The components $w_1(r,\chi_p,\theta_l,\phi_j)$ for $j = 2,4,6 \dots N_\phi$ are samples of the received signal in the upper sphere for $\phi = \delta\phi, 3\delta\phi, 5\delta\phi \dots 2\pi - \delta\phi$, respectively, multiplied by -1, and they thus represent the negatives of the samples of the received signal in the left-hand side of (6).

Let us now form an analytical, continuous signal as follows:

$$w_1(r,\chi,\theta,\phi) = \sum_{m=-M}^{M} \left(w^{(e)}_m(r,\chi,\theta) e^{-iK(m)N'_\phi\phi} + w^{(o)}_m(r,\chi,\theta) \right) e^{im\phi} \tag{13}$$

where

$$K(m) = \begin{cases} -1 & (m < 0) \\ 1 & (m \geq 0). \end{cases}$$

Importantly, the components $w_1(r,\chi_p,\theta_l,\phi_j)$ of the discrete signal in (11) now represent samples of the signal in (13) for $\chi = \chi_p$ and $\theta = \theta_l$ for all indices $j = 1 \dots N_\phi$. Equation (13) is further written as

$$\begin{aligned} w_1(r,\chi,\theta,\phi) &= w^{(e)}_0(r,\chi,\theta) e^{-iN'_\phi\phi} + w^{(o)}_0(r,\chi,\theta) \\ &\quad + \sum_{m=1}^{M} \left(w^{(e)}_m(r,\chi,\theta) e^{i(m-N'_\phi)\phi} + w^{(o)}_m(r,\chi,\theta) e^{im\phi} \right. \\ &\quad \left. + w^{(e)}_{-m}(r,\chi,\theta) e^{-i(m-N'_\phi)\phi} + w^{(o)}_{-m}(r,\chi,\theta) e^{-im\phi} \right). \end{aligned} \tag{14}$$

The signal in (14) is periodic, with the period of 2π, and bandlimited, and it may be written as the following Fourier expansion:

$$w_1(r,\chi,\theta,\phi) = \sum_{m=-N'_\phi}^{N'_\phi - 1} c_m(r,\chi,\theta) e^{im\phi} \tag{15}$$

where, see (16), shown at the bottom of the page, and where $N'_\phi \geq M+1$ is assumed, and

$$\begin{cases} M' = N'_\phi - M \\ M_0 = \min(M'-1, M) \\ M_1 = \max(M+1, M') \end{cases}. \tag{17}$$

The discrete signals in (11) consist of the samples of the signal in (15) equidistantly spaced in ϕ for $\chi = \chi_p$ and $\theta = \theta_l$. Therefore, performing the IDFT of the discrete signal in (11) now leads to the solutions for the Fourier coefficients $c_m(r,\chi_p,\theta_l)$ in (16). The IDFT is defined here as follows:

$$[c_m(r,\chi_p,\theta_l) | m = 0 \dots N'_\phi - 1, -N'_\phi \dots -1] = \text{IDFT}[\bar{w}_{pl}]. \tag{18}$$

The essential, useful property of the double ϕ-step θ-scanning technique, which leads to the crucial computational advantages in the probe correction for arbitrary probes, is shown in (16). For example, with the choice $N'_\phi = M+1$, one obtains: $M' = 1, M_0 = 0$ and $M_1 = N'_\phi$. Then, for

$$c_m(r,\chi,\theta) = \begin{cases} w^{(e)}_{m+N'_\phi}(r,\chi,\theta) & (-N'_\phi \leq m \leq -M_1) \\ 0 & (-M' < m < -M) \\ w^{(o)}_m(r,\chi,\theta) + w^{(e)}_{m+N'_\phi}(r,\chi,\theta) & (-M \leq m \leq -M') \\ w^{(o)}_m(r,\chi,\theta) & (-M_0 \leq m \leq M_0) \\ w^{(o)}_m(r,\chi,\theta) + w^{(e)}_{m-N'_\phi}(r,\chi,\theta) & (M' \leq m \leq M) \\ 0 & (M < m < M') \\ w^{(e)}_{m-N'_\phi}(r,\chi,\theta) & (M_1 \leq m \leq N'_\phi - 1) \end{cases} \tag{16}$$

a fixed m for $1 \leq m \leq M$, the known Fourier coefficient $c_m(r,\chi,\theta)$ is a sum of only $w_m^{(o)}(r,\chi,\theta)$ and $w_{m-N'_\phi}^{(e)}(r,\chi,\theta)$ whereas the known Fourier coefficient $c_{m-N'_\phi}(r,\chi,\theta)$ is a sum of only $w_{m-N'_\phi}^{(o)}(r,\chi,\theta)$ and $w_m^{(e)}(r,\chi,\theta)$. For $m=0$ the known Fourier coefficient $c_m(r,\chi,\theta)$ is equal to $w_m^{(o)}(r,\chi,\theta)$ whereas the known Fourier coefficient $c_{m-N'_\phi}(r,\chi,\theta)$ is equal to $w_m^{(e)}(r,\chi,\theta)$. In other words, this mixing of the Fourier coefficients of the even and odd-order signals occurring in the IDFT of the double ϕ-step θ-scan signals is relatively simple, and this enables the exploitation of the orthogonality of $e^{im\phi}$ indirectly. It is noted, though without presenting a proof here, that this mixing of the Fourier coefficients of the even and odd-order signals is crucially more complex in the case of the θ scanning with an arbitrary probe.

3) Matrix Inversions: The second step of the probe correction based on the double ϕ-step θ-scanning technique comprises matrix inversions, and it will be described now. An equation pair valid for all values of $N'_\phi \geq M+1$ is first written from (16) as follows:

$$\begin{cases} c_m(r,\chi,\theta) = I(M-m)w_m^{(o)}(r,\chi,\theta) \\ \qquad\qquad +I(m-M')w_{m'}^{(e)}(r,\chi,\theta) \\ c_{m'}(r,\chi,\theta) = I(M-m)w_m^{(e)}(r,\chi,\theta) \\ \qquad\qquad +I(m-M')w_{m'}^{(o)}(r,\chi,\theta) \\ \qquad\qquad\qquad (0 \leq m \leq N'_\phi - 1) \end{cases} \tag{19}$$

where $m' = m - N'_\phi$, and

$$I(m) = \begin{cases} 0 & (m<0) \\ 1 & (m \geq 0) \end{cases}.$$

The left-hand side of this pair of equations is known from the IDFT performed in (18) for $\chi = \chi_p$ for $p = 1$ and 2, and for $\theta = \theta_l$ for $l = 1 \ldots N_\theta$. The pair of equations is now used together with (7) and (8) to build an over-determined system of linear equations for each fixed m for $0 \leq m \leq N'_\phi - 1$ as follows:

$$\begin{bmatrix} \bar{\bar{G}}_m^{(o)} \\ \bar{\bar{G}}_m^{(e)} \end{bmatrix} \bar{Q}_m = \begin{bmatrix} \bar{C}_m \\ \bar{C}_{m'} \end{bmatrix}, (0 \leq m \leq M_0) \tag{20}$$

$$\begin{bmatrix} \bar{\bar{G}}_m^{(o)} & \bar{\bar{G}}_{m'}^{(e)} \\ \bar{\bar{G}}_m^{(e)} & \bar{\bar{G}}_{m'}^{(o)} \end{bmatrix} \begin{bmatrix} \bar{Q}_m \\ \bar{Q}_{m'} \end{bmatrix} = \begin{bmatrix} \bar{C}_m \\ \bar{C}_{m'} \end{bmatrix}, (M' \leq m \leq M) \tag{21}$$

$$\begin{bmatrix} \bar{\bar{G}}_{m'}^{(e)} \\ \bar{\bar{G}}_{m'}^{(o)} \end{bmatrix} \bar{Q}_{m'} = \begin{bmatrix} \bar{C}_m \\ \bar{C}_{m'} \end{bmatrix}. \ (M_1 \leq m \leq N'_\phi - 1). \tag{22}$$

Here, the matrices $\bar{\bar{G}}_m^{(\alpha)}$, where $\alpha = o \vee e$, are as follows:

$$\bar{\bar{G}}_m^{(\alpha)} = \begin{bmatrix} \bar{\bar{g}}_{11}^{(m,\alpha)} & \cdots & \bar{\bar{g}}_{1N'}^{(m,\alpha)} \\ \vdots & \vdots & \\ \bar{\bar{g}}_{N_\theta 1}^{(m,\alpha)} & \cdots & \bar{\bar{g}}_{N_\theta N'}^{(m,\alpha)} \end{bmatrix}, (-M \leq m \leq M) \tag{23}$$

where $N' = N - n_0 + 1$. For $l = 1 \ldots N_\theta$, and for $n' = 1 \ldots N'$, the block matrices $\bar{\bar{g}}_{ln'}^{(m,\alpha)}$ are

$$\bar{\bar{g}}_{ln'}^{(m,\alpha)} = \begin{bmatrix} g_{1mn}^{(\alpha)}(r,\chi_1,\theta_l) & g_{2mn}^{(\alpha)}(r,\chi_1,\theta_l) \\ g_{1mn}^{(\alpha)}(r,\chi_2,\theta_l) & g_{2mn}^{(\alpha)}(r,\chi_2,\theta_l) \end{bmatrix} \tag{24}$$

where the relation $n = n' + n_0 - 1$ holds, and where the values for the elements $g_{smn}^{(\alpha)}(r,\chi_p,\theta_l)$ for $s = 1$ and 2 are calculated from (9) and (10).

The $\bar{Q}_m$ and $\bar{Q}_{m'}$, and the $\bar{C}_m$ and $\bar{C}_{m'}$, shown in (20)–(22), are obtained from

$$\bar{Q}_m = \begin{bmatrix} Q_{1mn_0} \\ Q_{2mn_0} \\ \vdots \\ Q_{1mN} \\ Q_{2mN} \end{bmatrix}, (-M \leq m \leq M) \tag{25}$$

and

$$\bar{C}_m = \begin{bmatrix} c_m(r,\chi_1,\theta_1) \\ c_m(r,\chi_2,\theta_1) \\ \vdots \\ c_m(r,\chi_1,\theta_{N_\theta}) \\ c_m(r,\chi_2,\theta_{N_\theta}) \end{bmatrix}, (-M \leq m \leq M) \tag{26}$$

respectively.

Finally, the over-determined system of linear equations set up for each fixed m for $0 \leq m \leq N'_\phi - 1$ is solved by means of pseudo inversion [14]. For example, if $N'_\phi = M+1$, for $m = 0$ all coefficients Q_{s0n} ($s = 1$ and 2, $n = 1 \ldots N$) are found from (20), and for each fixed $m = 1 \ldots M$, all coefficients Q_{smn} ($s = 1$ and 2, $n = \max(1,|m|) \ldots N$) and $Q_{sm'n}$ ($s = 1$ and 2, $n = \max(1,|m'|) \ldots N$), where $m' = m - N'_\phi$, are found from (21). In this way all the desired coefficients Q_{smn} for $s = 1$ and 2, for $-M \leq m \leq M$, and for $n = \max(1,|m|) \ldots N$ are thus found.

IV. Validation

Computer calculations are carried out for validating the proposed double ϕ-step θ-scanning technique. The accuracy and the computational complexity of the probe correction technique based on the double ϕ-step θ-scanning technique is tested, and, for reference, compared with those of the general high-order probe correction technique based on the ϕ scanning.

A. Calculations

1) Probe Models: Two sets of probe receiving coefficients are used in the calculations, and these sets represent the probe models. For the first set, denoted by $\bar{R}^{(e)}$, the only non-zero coefficients are $R_{2\mu 1}^{(p)} = \mu/\sqrt{2}$ for $\mu = \pm 1$. This set represents an x'-oriented electric Hertzian dipole probe [1]. Another set of probe receiving coefficients, denoted by $\bar{R}^{(a)}$, is generated for $\sigma = 1,2$ for $\nu = 1 \ldots \nu_{\max}$, and for $\mu = -\min(\mu_{\max},\nu) \ldots \min(\mu_{\max},\nu)$, using $\nu_{\max} = 10$ and $\mu_{\max} = 5$, so that each coefficient is a random complex number $be^{i2\pi c}$. The b and c are random numbers between 0 and 1. This set represents an arbitrary probe.

2) AUT Models: In total 12 sets of spherical vector wave coefficients are generated for $s = 1, 2$, for $n = 1 \ldots N$, and for $m = -\min(M, n) \ldots \min(M, n)$, so that each coefficient is represented by a random complex number $be^{i2\pi c}$ (with unit $\sqrt{W}$ [1]). The 12 sets are obtained by varying $N = 40, 80, 160, 320$ so that for each fixed N, the M is varied as $M = N/4, N/2, N$. These sets, denoted by $\bar{Q}_{N,M}$, are used as reference sets later in this paper, and they represent the radiated fields of AUTs of different electrical size. For example, the case with $N = 320$ corresponds to a case where the radius of the AUT minimum sphere is approximately 50 λ, and the number of coefficients in $\bar{Q}_{N,M}$ with $N = M = 320$ exceeds 2×10^5.

3) Calculation of the Double ϕ-Step θ-Scan Signals: Using the sets $\bar{R}^{(e)}$ and $\bar{R}^{(a)}$, and $\bar{Q}_{N,M}$ for each combination of N and M, and by choosing the parameters values $N'_\theta = 2(N+1)$ and $N'_\phi = M + 1$ according to the sampling criteria presented in Section III-B.1, the received signal is calculated in the directions (θ, ϕ) and the probe orientation angles (χ) defined in Section III-A for the measurement distance $r = (2/k)(\nu_{\max} + N)$. The signals then become available in the upper sphere in a similar grid as illustrated in Fig. 3, that is, for every second ϕ angle the signals are available for $\chi = 0$ and $\pi/2$ whereas for the other ϕ angles the signals are available for $\chi = \pi$ and $3\pi/2$.

4) Calculation of the ϕ-Scan Signals: Using the sets $\bar{R}^{(e)}$ and $\bar{R}^{(a)}$ and $\bar{Q}_{N,M}$, the received signal is calculated in the same directions (θ, ϕ) in the upper sphere, and for the same measurement distance, as for the double ϕ-step θ-scanning technique, but for the probe orientation angles $\chi = 0$ and $\pi/2$ in each direction. This corresponds to the ϕ scanning [1].

5) Application of the Probe Correction Techniques: Finally, the probe correction technique presented in Section III-B is applied by using the double ϕ-step θ-scan signals, and the general high-order probe correction technique [5] by using the ϕ-scan signals. These calculations thus provide 48 sets of spherical vector wave coefficients in total (2 probe models, 12 AUT models, and 2 probe correction techniques), and these sets are denoted by $\bar{Q}^{(\kappa,\xi)}_{N,M}$, where $\kappa = d$ for the probe correction technique based on the double ϕ-step θ-scanning technique, $\kappa = g$ for the general high-order probe correction technique, $\xi = e$ for the electric Hertzian dipole probe $(\bar{R}^{(e)})$, and $\xi = a$ for the arbitrary probe $(\bar{R}^{(a)})$.

B. Results

1) Accuracy: The accuracy of the probe correction technique based on the double ϕ-step θ-scanning technique, and for reference that of also the general high-order probe correction technique, are tested by comparing the sets $\bar{Q}^{(\kappa,\xi)}_{N,M}$ with the reference set $\bar{Q}_{N,M}$. The difference set $\bar{\epsilon}^{(\kappa,\xi)}_{N,M} = \bar{Q}^{(\kappa,\xi)}_{N,M} - \bar{Q}_{N,M}$ is calculated first via component by component subtraction. The maximum relative difference, $\gamma^{(\kappa,\xi)}_{N,M}$, is then calculated from

$$\gamma^{(\kappa,\xi)}_{N,M} = 20\log_{10}\left(\frac{\max\left[\left|\bar{\epsilon}^{(\kappa,\xi)}_{N,M}\right|\right]}{\max[|\bar{Q}_{N,M}|]}\right) \tag{27}$$

TABLE I
THE VALUES OF $\gamma^{(\kappa,\xi)}_{N,M}$ [dB] FOR THE ARBITRARY PROBE $(\xi = a)$

	$N=40$		$N=80$		$N=160$		$N=320$	
M	$\kappa=d$	$\kappa=g$	$\kappa=d$	$\kappa=g$	$\kappa=d$	$\kappa=g$	$\kappa=d$	$\kappa=g$
$\frac{N}{4}$	−265	−258	−251	−247	−236	−215	−187	−183
$\frac{N}{2}$	−259	−261	−247	−243	−239	−217	−229	−180
N	−263	−260	−240	−245	−209	−217	−163	−184

TABLE II
THE VALUES OF $\gamma^{(\kappa,\xi)}_{N,M}$ [dB] FOR THE ELECTRIC HERTZIAN DIPOLE PROBE $(\xi = e)$

	$N=40$		$N=80$		$N=160$		$N=320$	
M	$\kappa=d$	$\kappa=g$	$\kappa=d$	$\kappa=g$	$\kappa=d$	$\kappa=g$	$\kappa=d$	$\kappa=g$
$\frac{N}{4}$	−282	−281	−275	−275	−270	−270	−264	−263
$\frac{N}{2}$	−280	−280	−275	−275	−268	−268	−262	−262
N	−279	−279	−272	−272	−266	−266	−257	−257

TABLE III
THE VALUES OF τ [dB] FOR THE CASE WITH THE ARBITRARY PROBE

	$N=40$		$N=80$		$N=160$		$N=320$	
M	$\kappa=d$	$\kappa=g$	$\kappa=d$	$\kappa=g$	$\kappa=d$	$\kappa=g$	$\kappa=d$	$\kappa=g$
$\frac{N}{4}$	0.77	−1.42	5.00	2.81	8.87	7.03	12.96	11.03
$\frac{N}{2}$	1.08	−0.64	5.48	3.27	9.51	7.56	13.47	11.53
N	0.87	−0.42	4.93	3.43	8.92	7.68	12.92	11.69

where the $\max[|\bar{\epsilon}^{(\kappa,\xi)}_{N,M}|]$ and $\max[|\bar{Q}_{N,M}|]$ are the maximum values of the absolute values of the coefficients of the sets $\bar{\epsilon}^{(\kappa,\xi)}_{N,M}$ and $\bar{Q}_{N,M}$, respectively.

The obtained $\gamma^{(\kappa,\xi)}_{N,M}$ values for the arbitrary probe $(\xi = a)$ and for the electric Hertzian dipole probe $(\xi = e)$ are presented in Tables I and Table II, respectively. The values of $\gamma^{(\kappa,\xi)}_{N,M}$ are small for the range $40 \le N \le 320$ for all M, and they are likely due to numerical inaccuracies in the calculations. The values, however, increase with increasing N the increase rate being significantly higher for the arbitrary probe compared to the electric Hertzian dipole probe. This indicates that the numerical inaccuracies depend on the probe. Nevertheless, in conclusion, the probe correction technique based on the double ϕ-step θ-scanning technique works and provides an accuracy that is comparable to that of the general high-order probe correction technique.

2) Computational Complexity: The central processing unit (CPU) times for performing the required pseudo-inverse operations for the two probe correction techniques for each combination of N and M were recorded during the calculations. The values of τ, where the τ is related to the CPU time in seconds, T, as $\tau = \log_2(T)$, are shown in Table III for the case with the arbitrary probe.

The main result shown in Table III is that the values of τ are increased by a factor of approximately 4, and thus T by a factor of approximately 16, as N is doubled. This indicates that the computational complexity for both probe correction techniques is $O(N^4)$. Furthermore, the results in Table III show that, for $M = (N/2)$ and $N/4$ the required CPU time for the probe correction technique based on the double ϕ-step θ-scanning technique is higher by a factor of approximately 4 compared to that for the general high-order probe correction technique. For $M = N$ this factor is approximately 2.5. For the case with $N = M = 320$, the actual CPU times for performing

the required pseudo-inverse operations (on a typical personal computer of today) for the probe correction techniques based on the double ϕ-step θ-scanning technique and for the general high-order probe correction techniques were approximately 130 and 55 minutes, respectively. It is noted, that parallel computing can be easily exploited in the data processing related to both probe correction techniques.

V. Conclusion

The double ϕ-step θ-scanning technique for spherical near-field antenna measurements has been introduced. This technique constitutes an alternative scanning technique for spherical near-field antenna measurements. Compared to the (usual) θ-scanning technique [1] the double ϕ-step θ-scanning technique doubles the ϕ increment and, instead of stepping from 0 to π, steps from 0 to 2π in ϕ. Therefore, the overall measurement time for the two scanning techniques does not differ significantly.

In the case of the ϕ and θ scanning techniques [1], the obtainable computational complexity of the probe correction is $O(N^3)$ for a first-order probe, and it is $O(N^4)$ for an odd-order probe [3]. However, in the case of an arbitrary probe, the computational complexity is $O(N^4)$ for the ϕ scanning [5] while it becomes $O(N^6)$ for the θ scanning. The important insight of this paper is that the application of the introduced double ϕ-step θ-scanning technique with an arbitrary probe enables formulating a probe correction technique with the computational complexity of $O(N^4)$. The formulation of this probe correction technique has been presented in the paper. Thus, for arbitrary probes, the double ϕ-step θ-scanning technique and the associated probe correction technique provide a method to benefit from the practical advantages of the θ scanning over the ϕ scanning without crucially compromising with the computational complexity of the probe correction.

The probe correction technique based on the double ϕ-step θ-scanning technique has been shown to work by computer calculations in this paper. The technique has been tested also against numerically generated noise and truncation errors, and shown to work.

Acknowledgment

The author wants to thank European Space Agency for the financial support of this work. The author wants to thank also his closest colleagues in the Technical University of Denmark, in particular Jeppe Majlund Nielsen, Sergey Pivnenko and Olav Breinbjerg for creating an inspiring environment for making the necessary research findings for this paper.

References

[1] J. E. Hansen, *Spherical Near-Field Antenna Measurements*. London, U.K.: Peter Peregrinus, 1988.

[2] A. D. Yaghjian, "An overview of near-field antenna measurements," *IEEE Trans. Antennas Propag.*, vol. 34, no. 1, pp. 30–45, Jan. 1986.

[3] T. A. Laitinen, S. Pivnenko, and O. Breinbjerg, "Odd-order probe correction technique for spherical near-field antenna measurements," *Radio Sci.*, vol. 40, no. 5, pp. 3009–3019, June 2005.

[4] T. A. Laitinen, S. Pivnenko, and O. Breinbjerg, "Iterative probe correction technique for spherical near-field antenna measurements," *IEEE Antennas Wireless Propag. Lett.*, vol. 4, pp. 221–223, 2005.

[5] T. A. Laitinen, S. Pivnenko, and O. Breinbjerg, "High-order probe correction for a square waveguide probe in spherical near-field antenna measurements," in *Proc. AMTA Europe Symp.*, Munich, Germany, May 2006, pp. 187–192.

[6] T. A. Laitinen, S. Pivnenko, and O. Breinbjerg, "Application of the iterative probe correction technique for a high-order probe in spherical near-field antenna measurements," *IEEE Antennas Propag. Mag.*, vol. 48, pp. 179–185, Aug. 2006.

[7] DTU-ESA Spherical Near-Field Antenna Test Facility Technical University of Denmark, 2006 [Online]. Available: http://www.oersted.dtu.dk/English/research/es/afg/dtu_esa_facility.aspx

[8] T. A. Laitinen, S. Pivnenko, J. Nielsen, and O. Breinbjerg, Development of 1–3 GHz Probes for the DTU-ESA Spherical Near-Field Antenna Test Facility. ESTEC Contract No. 18222/04/NL/LvH/bj. Final Report, Volume 1: Executive Summary Denmark: Electromagnetic Systems ØDTU, Tech. Univ. Denmark, Lyngby, report R 729, Nov. 2006.

[9] T. A. Laitinen, S. Pivnenko, J. Nielsen, and O. Breinbjerg, "Practical aspects of spherical near-field antenna measurements using a high-order probe," presented at the 1st Eur. Conf. Antennas and Propagation (EuCAP'06), Nice, France, Nov. 6–10, 2006, no. ISBN 92-9092-9375,.

[10] O. M. Bucci, F. D'Agostino, C. Gennarelli, G. Riccio, and C. Savarese, "Near-field-far-field transformation with spherical spiral scanning," *IEEE Antennas Wireless Propag. Lett.*, vol. 2, pp. 263–266, 2003.

[11] R. L. Lewis and R. C. Wittmann, "Improved spherical and hemispherical scanning algorithms," *IEEE Trans. Antennas Propag.*, vol. 35, no. 12, pp. 1381–1388, Dec. 1987.

[12] R. C. Wittmann, B. K. Alpert, and M. H. Francis, "Near-field, spherical-scanning antenna measurements with nonideal probe locations," *IEEE Trans. Antennas Propag.*, vol. 52, no. 8, pp. 2184–2186, Aug. 2004.

[13] R. C. Baird, A. C. Newell, and C. F. Stubenrauch, "A brief history of near-field measurements of antenna at the national bureau of standards," *IEEE Trans. Antennas Propag.*, vol. 36, no. 6, pp. 727–733, 1988.

[14] S. L. Campbell and C. D. Meyer, *Generalized Inverses of Linear Transformations*. New York: Dover, 1991.

Tommi Laitinen was born in Pihtipudas, Finland, on March 19, 1972. He received the Master of Science in Technology, the Licentiate of Science in Technology, and the Doctor of Science in Technology degrees in electrical engineering from Helsinki University of Technology (TKK), Espoo, Finland, in 1998, 2000, and 2005, respectively.

His major research interests at TKK were small antenna measurements. From 2003 until the end of 2006, he was with the Technical University of Denmark (DTU) as a Postdoctoral Researcher and Assistant Professor. His research interests at DTU were spherical near-field antenna measurements. During these years, he mainly contributed to the development of an accurate antenna pattern characterization procedure for the DTU-ESA Spherical Near-Field Antenna Test Facility based on spherical near-field antenna measurements with a high-order probe. Since the beginning of 2007, he has been with the Radio Laboratory, TKK, as a Senior Researcher. While carrying on with his research on spherical near-field antenna measurements, he also works with small antenna measurements, sensor applications and related radio-frequency electronics. His other duties at TKK include occasionally teaching master's and postgraduate courses. He is the author or coauthor of approximately 40 journal papers, conference papers, or technical reports, mainly in the field of antenna measurements.

Dr. Laitinen authored a paper that was selected among the best student papers in the 1999 Antenna Measurement Techniques Association (AMTA) conference, and another conference paper authored by him was selected among the best papers in the 2005 AMTA conference. He has been a Reviewer for conferences and international scientific journals, such as the IEEE Transactions on Antennas and Propagation.